46 Blumwald, E. and Gelli, A. (1997) Secondary inorganic ion transport at the tonoplast, *Adv. Bot. Res.* 25, 401–417
47 Gaxiola, R.A. *et al*. (1999) The *Arabidopsis thaliana* proton transporters, AtNhx1 and Avp1, can function in cation detoxification in yeast, *Proc. Natl. Acad. Sci. U. S. A.* 96, 1480–1485
48 Nass, R., Cunningham, K.W. and Rao, R. (1997) Intracellular sequestration of sodium by a novel Na^+/H^+ exchanger in yeast is enhanced by mutations in the plasma membrane H^+-ATPase, *J. Biol. Chem.* 272, 26145–26152
49 Prior, C. *et al*. (1996) Characterization of the *NHA1* gene encoding a Na^+/H^+-antiporter of the yeast *Saccharomyces cerevisiae*, *FEBS Lett.* 387, 89–93
50 Haro, R., Garciadeblas, B. and Rodriguez-Navarro, A. (1991) A novel P-type ATPase from yeast involved in sodium transport, *FEBS Lett.* 291, 189–191
51 Axelsen, K.B. and Palmgren, M.G. (1998) Evolution of substrate specificities in the P-type ATPase superfamily, *J. Mol. Evol.* 46, 84–101
52 Haro, R. *et al*. (1993) Genetic basis of sodium exclusion and sodium tolerance in yeast. A model for plants, *Physiol. Plant.* 89, 868–874
53 Rios, G., Ferrando, A. and Serrano, R. (1997) Mechanisms of salt tolerance conferred by overexpression of the *HAL1* gene in *Saccharomyces cerevisiae*, *Yeast* 13, 515–528
54 Garciadeblas, B. *et al*. (1993) Differential expression of two genes encoding isoforms of the ATPase involved in sodium efflux in *Saccharomyces cerevisiae*, *Mol. Gen. Genet.* 236, 363–368
55 Bressan, R.A., Hawegawa, P.M. and Pardo, J.M. (1998) Plants use calcium to resolve salt stress, *Trends Plant Sci.* 3, 411–412
56 Liu, J. and Zhu, J.K. (1997) An *Arabidopsis* mutant that requires increased calcium for potassium nutrition and salt tolerance, *Proc. Natl. Acad. Sci. U. S. A.* 94, 14960–14964
57 Liu, J. and Zhu, J.K. (1998) A calcium sensor homolog required for plant salt tolerance, *Science* 280, 1943–1945
58 Pardo, J.M. *et al*. (1998) Stress signaling through Ca^{2+}/calmodulin-dependent protein phosphatase calcineurin mediates salt adaptation in plants, *Proc. Natl. Acad. Sci. U. S. A.* 95, 9681–9686

Daniel Schachtman* and Weihong Liu are at the CSIRO Plant Industry – Horticulture Unit, GPO Box 350, Glen Osmond, SA 5064, Australia.

*Author for correspondence (tel +61 8 83038628; fax +61 8 83038601; e-mail daniel.schachtman@pi.csiro.au).

technical focus

GFP-based FRET microscopy in living plant cells

The fate and function of biomolecules in living plant cells is a challenging area of plant science. On the one hand, *in vitro* studies on isolated biomolecules are often difficult to extrapolate to *in vivo* function because of the complex organization and high degree of compartmentalization in living plant cells. On the other hand, the *in vivo* study of molecular function is technically demanding, as it requires the simultaneous capability of detecting molecules with high (subcellular) spatial resolution, high sensitivity, high specificity and yet with minimal perturbation of the cell state, in addition to obtaining information about the molecular state or molecular environment. The combination of green fluorescent protein (GFP) technology with fluorescence resonance energy transfer (FRET) microscopy offers these capabilities, and thereby creates new horizons for molecular plant cell biology, particularly in the field of signal transduction.

GFP and chromophore mutants

The GFP from the jellyfish *Aequorea victorea* is a 21 kDa apo-protein that spontaneously folds into a bright-green fluorescing structure. The gene encoding GFP can be expressed in many (non-jellyfish) cell types, enabling the use of GFP as a molecular marker for gene expression.

By fusing the gene encoding GFP with a gene encoding an endogenous protein, and the subsequent expression of the chimera, fluorescent fusion proteins can be produced and targeted to specific subcellular organelles. Consequently, the fate of these fusion proteins and the organelle dynamics can be monitored in living plants at the single cell level with

Box 1. Chromophore mutants of the green fluorescent protein (GFP)[a]

Essential amino acid substitutions, the resulting changed chemistry of the chromophore and the wavelengths for maximal absorbance and fluorescence are indicated.

- **Enhanced green fluorescent protein** (EGFP)
  Ser65 to Thr, Phe64 to Leu.
  Phenolate anion in chromophore.
  Absorbance/emission = 488/509 nm.
- **Yellow fluorescent protein** (YFP)
  Ser65 to Gly, Ser72 to Ala, Thr203 to Tyr.
  Phenolate anion in chromophore with stacked π-electron system (to Tyr203).
  Absorbance/emission = 514/527 nm.
  The addition of Val68 to Leu, Gln69 to Lys to YFP yields a more pH-insensitive (above pH 6.8) enhanced version of YFP with slightly red-shifted spectral properties:
  Absorbance/emission = 516/529 nm (Ref. 15).
- **Blue fluorescent protein** (BFP)
  Tyr66 to His, Tyr145 to Phe.
  Imidazole in chromophore.
  Absorbance/emission = 382/446 nm.
- **Cyan fluorescent protein** (CFP)
  Phe64 to Leu, Ser65 to Thr, Tyr66 to Trp, Asn146 to Ile, Met153 to Thr, Val163 to Ala, Asn212 to Lys.
  Indole in chromophore.
  Absorbance/emission = 434, 452/476, 505 nm.

[a]Some of the chromophore mutants of GFP are known under different names. Therefore, the abbreviations used here refer to chromophore mutant classes. For an overview of GFP chromophore mutants see Ref. 5.

1360 - 1385/99/$ – see front matter PII: S1360-1385(99)01426-0

Box 2. How can FRET be quantified experimentally?

- The donor fluorescence intensity (or quantum yield) is reduced:

$$E = 1 - \frac{I_{D,+A}}{I_{D,-A}}$$

($I_{D,+A}$ Donor fluorescence in the presence of the acceptor; $I_{D,-A}$ donor fluorescence in the absence of the acceptor).

- The donor fluorescence lifetime (τ) is reduced:

$$E = 1 - \frac{\tau_{D,+A}}{\tau_{D,-A}}$$

($\tau_{D,+A}$ donor fluorescence lifetime in the presence of the acceptor; $\tau_{D,-A}$ donor fluorescence lifetime in the absence of the acceptor).

- The acceptor (if fluorescent) becomes more fluorescent (sensitized):

$$E = \frac{\varepsilon_A}{\varepsilon_D}\left(\frac{I_{A,+D}}{I_{A,-D}} - 1\right)$$

($I_{A,+D}$ acceptor fluorescence in the presence of the donor; $I_{A,-D}$ acceptor fluorescence in the absence of the donor; ϵ_D and ϵ_A are the extinction coefficients of the donor and acceptor at a wavelength where both the donor and acceptor absorb. Note that donor fluorescence must be subtracted to get $I_{A,+D}$).

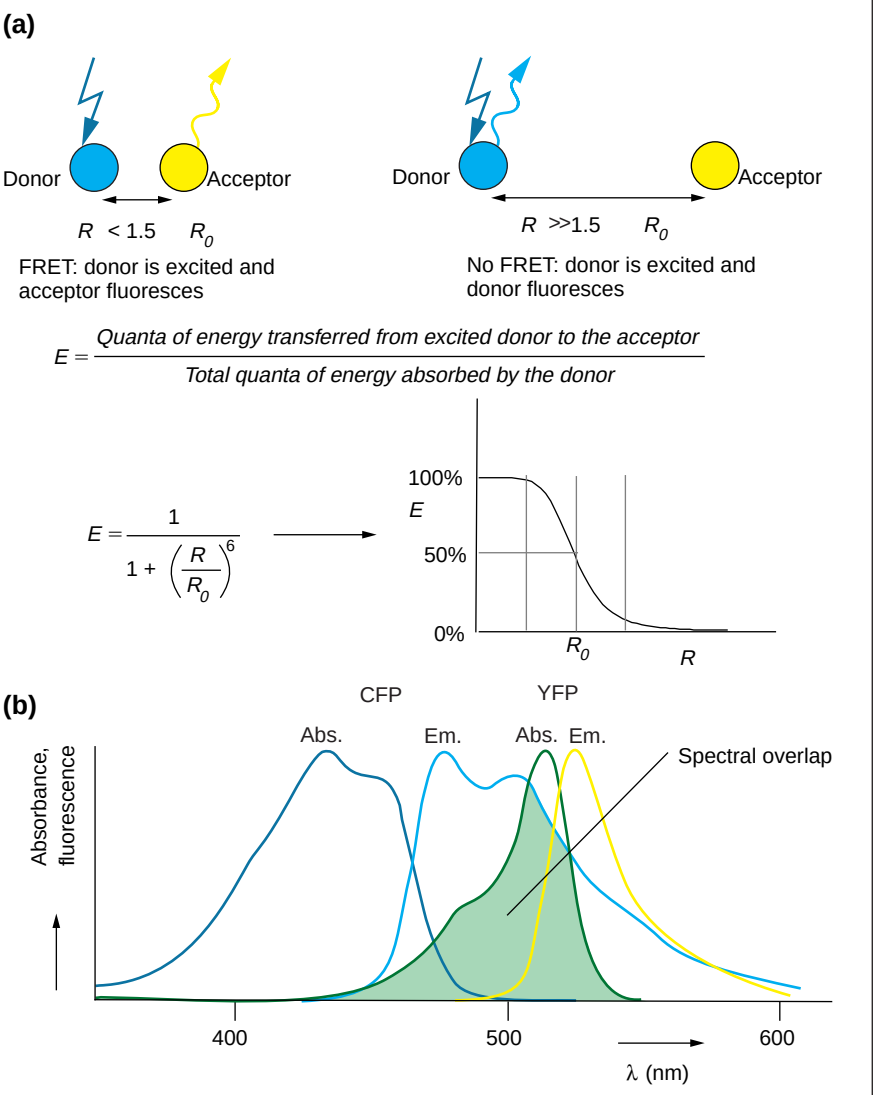

Fig. 1. (a) Definition of fluorescence resonance energy transfer (FRET) and its relation to donor– acceptor proximity. R_0 = the Förster radius for energy transfer, generally between 30–60 Å. The R_0 value is the distance between donor and acceptor at which the FRET efficiency (E) is 50% (i.e. 50% of the excitation energy absorbed by the donor is transferred to the acceptor). When donor and acceptor are separated by $1.5 \times R_0$ or more, the FRET efficiency is dropped to <8%. When donor and acceptor are separated by $<0.5 \times R_0$, the FRET efficiency is >98.5%. For this reason, FRET provides an excellent way of studying whether molecules indeed interact. (b) Prerequisites for FRET: (1) donor must be fluorescent; (2) there must be a spectral overlap between donor fluorescence and acceptor absorbance [the spectral overlap for the cyan fluorescent protein (CFP) and the yellow fluorescent protein (YFP) is indicated in green; Abs., absorbance; Em., emission]; (3) the distance between donor and acceptor must be $<2 \times R_0$; (4) the angle between donor and acceptor transition moments should not be 90° ($\kappa^2 \neq 0$, where κ^2 = the dipole orientation factor). See Refs 7,8 for a quantitative description of R_0.

high specificity, sensitivity and spatial resolution, and with minimal perturbation of the cell. For example, the recent studies of Golgi-stack movements along endoplasmic reticulum strands[1] and the successful use of GFP-fusion proteins for studying the dynamics of the actin[2] and tubulin[3] cytoskeleton in living plant cells.

Nowadays, as a result of site-directed mutagenesis, GFPs come in many flavours, fluorescing at different colours, and codon usage has been optimized for plants (eliminating a cryptic splice site)[4]. The chromophore of the wild-type GFP is formed from three amino acids (Ser65, Tyr66, Gly67) and mainly absorbs UV (397 nm) but also blue light (475 nm), and emits green fluorescence (505 nm). The most employed mutants are the enhanced green fluorescent protein, EGFP, which lacks the UV absorption of wild-type GFP; the blue fluorescent protein, BFP; the cyan fluorescent protein, CFP; and the most red-shifted, the yellow fluorescent protein, YFP (Box 1).

In line with the applications mentioned already, the spectroscopic mutants of GFP can be used to perform double labelling or co-localization studies[6]. But the use of fluorescence resonance energy transfer (FRET) between these different GFPs is far more powerful, enabling the study of protein–protein interactions, protein conformational changes and proteolytic processing with high (subcellular) resolution and sensitivity in living cells.

The FRET principle

FRET is the phenomenon whereby a fluorescent molecule – the donor –transfers energy by a nonradiative (through space) mechanism to a neighbouring chromophore – the acceptor (Fig. 1 and Box 2; for reviews see Refs 7,8). The absorption spectrum of the acceptor chromophore must overlap with the fluorescence emission spectrum of the donor. When the spectral overlap is more extensive, the efficiency of the FRET process will be higher and consequently, FRET can occur over longer distances. FRET is highly dependent on the proximity between the donor and acceptor,

and, in general, only occurs when the molecules are separated by <100 Å. It is characterized by the Förster radius (R_0; Fig. 1). R_0 values for common donor–acceptor pairs (reviewed in Ref. 7) usually vary between 30 and 60 Å and can be determined experimentally. They depend on the spectral overlap, the relative orientation of the donor and acceptor chromophores, and the quantum yield of the donor fluorophore[8].

Chromophore-mutated GFPs show an excellent spectral overlap and, hence, good FRET pairs can be made using the available GFPs (Ref. 9). For example, the BFP is a good donor to the Ser65 to Thr-mutated EGFP. The R_0 value for this pair is 40–43 Å depending on the exact amino acid substitutions[5]. Superior to the BFP–GFP pair is the use of the CFP–YFP pair, with an R_0 value of 49–52 Å depending on the choice of the types of CFP and YFP (Ref. 5). With such high R_0 values, even at a separation of 80 Å between CFP and YFP, a 10% FRET efficiency can be observed. Furthermore, with the CFP–YFP FRET pair, cytotoxic UV excitation (required for the BFP–GFP pair) can be avoided.

FRET measurement

FRET is manifested by a decrease in the fluorescence intensity (or quantum yield) of the donor fluorophore. If the acceptor chromophore is a fluorophore, FRET will increase the fluorescence of the acceptor (the so-called sensitized emission). With digital imaging techniques it is possible to quantify the altered ratio of donor:acceptor fluorescence and to determine the FRET efficiency. However, the ratio of the measured donor:acceptor fluorescence intensity also depends on the microscope optics and the local relative concentrations of the donor and acceptor. Therefore the actual microscopic FRET measurements are rather complex, requiring (at least) three separate images, collected at different excitation and emission filter–wavelength combinations, and several instrumental correction factors[10]. For many plant cell types another complicating factor is the direct absorption (or filtering) of fluorescence by chlorophyll pigments, which decreases blue fluorescence intensity (such as for BFP and CFP), which can be misinterpreted as a reduced donor-fluorescence quantum yield caused by FRET.

FRET also decreases the fluorescence lifetime (the average time that the molecule spends in the excited state) of the donor[8]. Unlike fluorescence intensity, the fluorescence lifetime (or τ) is not dependent on local chromophore concentration, direct absorption of donor fluorescence (e.g. by chlorophyll) or on (moderate levels of) photobleaching, and consequently provides quantitative information about the FRET efficiency. For this reason, fluorescence lifetime imaging microscopy

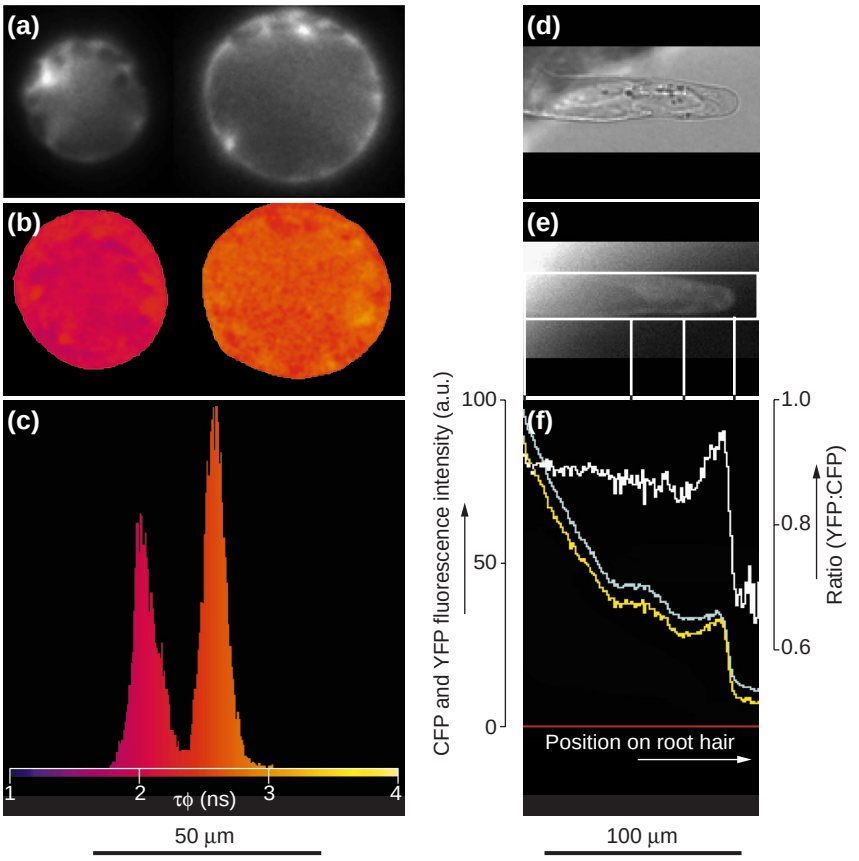

Fig. 2. Fluorescence resonance energy transfer (FRET) microscopy in yellow-cameleon. (a–c) Fluorescence lifetime imaging microscopy (FLIM) analysis of the cyan fluorescent protein (CFP) fluorescence of living Cowpea (*Vigna unguiculata*) mesophyll protoplasts expressing yellow-cameleon-2, a fusion protein containing both CFP and yellow fluorescent protein (YFP) (left protoplast) or expressing unfused cytosolic CFP (right protoplast). Only the CFP fluorescence emission is monitored. (a) Fluorescence intensity image, (b) fluorescence lifetime image, (c) temporal histogram and pseudocolour scale of the fluorescence lifetime pixel values of (b). The left protoplast was transfected with yellow-cameleon-2 (Ref. 14) under a modified 35S promoter using the pMON dicot expression vector as described in Ref. 13. The right protoplast was transfected using the same vector but containing only CFP (Phe64 to Leu, Ser65 to Thr, Tyr66 to Trp, Asn146 to Ile, Met153 to Thr, Val163 to Ala, Asn212 to Lys). The protoplasts were excited using the 457 nm argon-ion laser line modulated at 40 MHz, and the CFP fluorescence was selectively imaged using a 470–500 nm bandpass emission filter (the microscope setup, lifetime-image calculation and image processing are described in Ref. 13). From the pseudocoloured lifetime images, it can be inferred that the CFP lifetime of the cameleon-fusion protein is about 2.1 ns ($= 2.1 \times 10^{-9}$ s) whereas the CFP lifetime of unfused CFP is 2.6 ns. The reduced CFP lifetime in the yellow-cameleon is caused by intramolecular FRET, occurring at an efficiency of ~25% (Box 2). This example clearly shows that fluorescence lifetimes can be very accurately measured in living plant cells and that they are independent of the local fluorophore concentration. (d–f) Fluorescence spectral imaging microscopy (FSPIM) analysis of yellow-cameleon-2 expressed in root hairs of *Lotus japonicus*. (d) Phase contrast image of the root hair, (e) fluorescence intensity image and (f) the profile plots over the root hair axis of the CFP (cyan) and YFP (yellow) intensity and the YFP:CFP ratio (white). The roots were transformed using *Agrobacterium rhizogenes* carrying the yellow-cameleon-2 gene under the RH2 root epidermis-specific promoter. The root was excited using a mercury lamp and a 430–440 nm bandpass filter. The fluorescence emission was filtered through a 455 nm longpass filter and transferred on to a Chromex (Albuquerque, NM, USA) 250IS imaging spectrograph coupled to a Photometrics (Tucson, AZ, USA) CH250 CCD camera providing spatially resolved (along the root hair axis) fluorescence emission spectra. The entrance slit of the spectrograph is superimposed on (e). The CFP, YFP and autofluorescence spectral components were calculated from the multicomponent spectra using a linear four-component spectral-fitting procedure, similar to a procedure described in Ref. 16. The vertical lines drawn between (e) and (f) indicate the border of the entrance slit, the left and right borders of the nucleus and the tip of the root hair, respectively. As expected, the YFP:CFP fluorescence ratio, which is directly related to the cytosolic calcium concentration, is independent of the relative abundance of the fluorescent indicator. This can be seen by comparing the plot profiles of the CFP and YFP fluorescence intensity with the ratio plot profile.

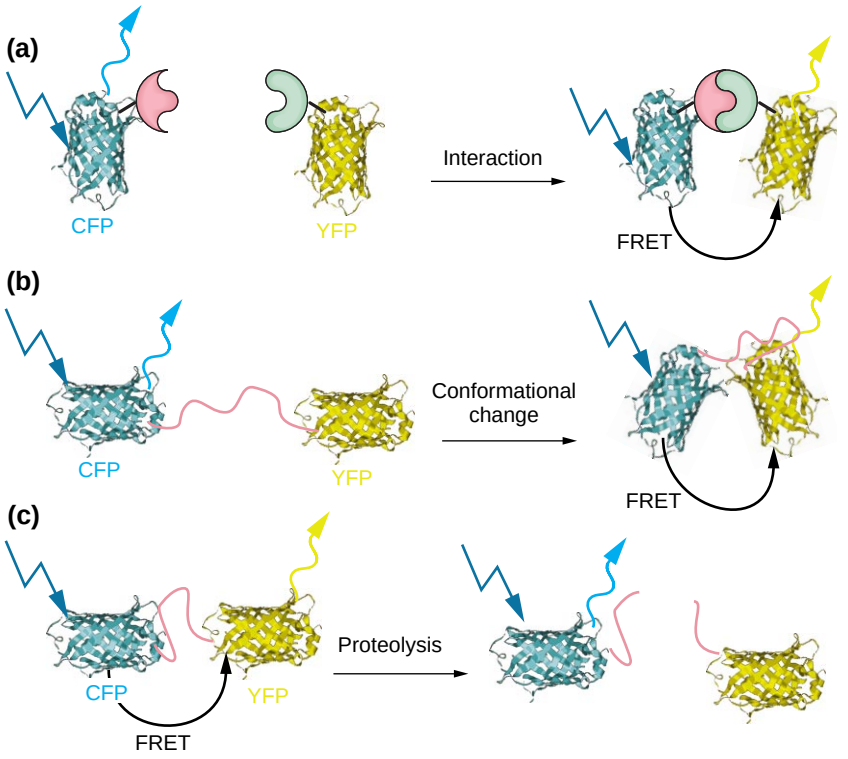

Fig. 3. Possible use of green fluorescent protein (GFP)-based fluorescence resonance energy transfer (FRET) microscopy indicators. (a) Protein–protein interactions. (b) Monitoring of the conformational state of fusion proteins. (c) Proteolytic cleavage of fusion proteins. Abbreviations: CFP, cyan fluorescent protein; YFP, yellow fluorescent protein; dark blue arrow indicates excitation; cyan and yellow arrows indicate fluorescence; non-CFP or YFP fusion-proteins are represented in pink and green.

(FLIM; Fig. 2), producing high resolution micrographs in which each pixel value represents the local fluorescence lifetime, is ideal for studying FRET in single cells[11–13].

Yellow-cameleon-2 fusion protein

The yellow-cameleon-2 fusion protein was developed as a calcium indicator[14]. In addition to CFP and YFP units at either end of the molecule, the fusion protein also contains the calcium-binding protein calmodulin and the M13 calmodulin-binding protein. Upon binding calcium to the calmodulin part of the molecule, the M13 unit binds to the calmodulin unit, inducing a significant change in the distance or relative orientation of the CFP and YFP cylinders at the ends of the molecule (Fig. 3b). As a result, the FRET efficiency from CFP to YFP increases upon calcium binding[14,15]. Because the acceptor:donor molecular ratio in cameleon is always 1:1 (because they are fused into one protein), the YFP:CFP fluorescence intensity ratio can be directly related to the cytosolic calcium concentration.

The yellow-cameleon indicator is responsive to calcium in living cells of intact plants (Fig. 2). The roots of *Lotus japonicus* have been transformed with the yellow-cameleon-2 construct and the CFP and YFP-fluorescing components measured as a function of distance over the axis of a young, growing root hair by fluorescence spectral imaging microscopy (FSPIM)[16]. Polar growth at the root hair tip is regulated by a local increased calcium concentration[17]. Indeed, the ratio of YFP:CFP fluorescence increases significantly towards the root hair tip (Fig. 2). This reflects an increased calcium concentration inducing an enhanced FRET efficiency in the cameleon molecule.

Outlook

Of course, GFP-based FRET indicators can be used for many other purposes (Fig. 3). Firstly and most importantly, FRET can be used for monitoring protein–protein interactions. Two separate fusion proteins – one containing CFP and the other, its putative interacting partner containing YFP – are co-expressed in the plant cell type of choice (i.e. by using appropriate promoters). If intermolecular FRET is detected, it provides direct proof of the close proximity (i.e. <80 Å) of the CFP and YFP cylinders and consequently of the existence of the protein–protein interaction. Because, in general, the relative abundance of donor and acceptor for co-transformations is unknown or variable depending on the subcellular location, FLIM would be the most suitable technique for studying intermolecular FRET (Refs 12,13). This strategy was successful for demonstrating the interaction between the CFP–calmodulin and the M13–YFP fusion proteins in mammalian cells[14], and the interaction between the Bcl-2 and the Bax mitochondrial proteins using BFP and GFP fusions[18].

The attractive features of the microscopic measurement of FRET, are that, in addition to studying whether proteins do interact, it is possible to determine:

- If the interaction changes with time (because the FRET measurement is non-destructive).
- To what extent the proteins do interact.
- Where they interact (which cell types and at what subcellular location).

Another advantage of the method is that researchers are no longer restricted to the artificial nuclear environment (in another species) as they are for the yeast two-hybrid screening method.

The second area of application is the study of molecular conformational changes, such as the yellow-cameleon[14,15]. The strategy is to construct a sandwich-like fusion of CFP, a protein of interest and YFP. It is essential that the protein of interest can be induced to undergo a conformational change that alters the proximity and/or relative orientation of the CFP and YFP cylinders, changing the intramolecular FRET efficiency. Ligand or ion-binding domains of receptors or channels are interesting protein candidates, or, for instance, protein sequences with a phosphorylation site. Using such fusion proteins, ligand- or ion-binding, or phosphorylation can be studied in living plant cells with high spatial resolution by monitoring (local) alterations in FRET-efficiency.

The third area of application is the study of proteolytic processing of proteins *in vivo*. Again, a tandem fusion of CFP–YFP (or BFP–GFP) and a protein of interest (or part thereof) is constructed[9]. When the protein of interest is intact, FRET can be observed, but as soon the protein becomes cleaved and the parts dissociate, FRET is lost. The approach has proved useful for studying proteolytic processing in living mammalian cells during apoptosis[19].

As with any technique there are potential sources that can introduce artefacts. For instance, the pH-sensitivity of some of the GFPs (especially the YFP with a pK of near 6.9) might cause problems, restricting their applicability to subcellular areas with a pH >7 (i.e. not in vacuoles). Recently, the pH sensitivity of YFP was reduced significantly by introducing an extra mutation (Gln69Arg)[15]. However, as described by others, the pH-sensitivity of certain GFP variants can be utilized to provide subcellular targetable pH-indicators[20]. Another obvious problem can

be the bulkiness of the CFP–YFP cylinders (20 × 30 Å), which might yield inactive or incorrectly folded fusion proteins. In spite of the many successful bioactive fusion GFP-proteins published to date, there is no guarantee that novel fusion proteins are biofunctional. Hence, the FRET-approach for monitoring protein–protein interactions outlined here must include separate checks for the biofunctionality of the interacting fusion proteins. This prohibits the use of the FRET method as a quick screening method like the yeast two-hybrid system.

The main advantage of the GFP-based FRET indicators is that they employ the machinery of the plant cell for their synthesis and subcellular targeting. By using cell-type-specific promoters and/or fusion to targeting-sequences, the indicators can be produced specifically in the cell type and subcellular location of choice. Hence the potential for studying dynamic cell biological processes, such as intracellular signalling, is much greater than for microinjected or passively loaded chemical fluorescent indicators, which are usually restricted to the cytoplasm of the outer cell layers of the plant. Therefore, in spite of the fact that the experiments shown in Figure 2 represent only the first described *in vivo* FRET measurements between CFP and YFP in plants, the future potential is extensive.

Acknowledgements

We gratefully acknowledge the kind donation of the yellow-cameleon-2 construct by Dr R.Y. Tsien (Howard Hughes Medical Institute, University of California, San Diego, USA). We thank Rossana Mirabella for transforming Lotus roots. T.W.J.G. is supported by the Royal Netherlands Academy of Arts and Sciences (KNAW) and G.N.M.v.d.K. is supported by the Foundation for Earth and Life Sciences (ALW) of The Netherlands Organization of Scientific Research (NWO).

Theodorus W.J. Gadella, Jr*, Gerard N.M. van der Krogt and Ton Bisseling
Laboratory for Molecular Biology, MicroSpectroscopy Centre, Wageningen University, Dreijenlaan 3, NL-6703 HA Wageningen, The Netherlands

*Author for correspondence
(tel +31 317 484284; fax +31 317 483584; e-mail dorus.gadella@laser.bc.wau.nl)

References

1 Boevink, P. *et al.* (1998) Stacks on tracks: the plant Golgi apparatus traffics on an actin/ER network, *Plant J.* 15, 441–447
2 Kost, B., Spielhofer, P. and Chua, N.H. (1998) A GFP-mouse talin fusion protein labels plant actin filaments *in vivo* and visualizes the actin cytoskeleton in growing pollen tubes, *Plant J.* 16, 393–401
3 Marc, J. *et al.* (1998) A GFP–MAP4 reporter gene for visualizing cortical microtubule rearrangements in living epidermal cells, *Plant Cell* 10, 1927–1940
4 Haseloff, J. *et al.* (1997) Removal of a cryptic intron and subcellular localization of green fluorescent protein are required to mark transgenic *Arabidopsis* plants brightly, *Proc. Natl. Acad. Sci. U. S. A.* 94, 2122–2127
5 Tsien, R.Y. (1998) The green fluorescent protein, *Annu. Rev. Biochem.* 67, 509–544
6 Ellenberg, J., Lippincott-Schwartz, J. and Presley, J.F. (1999) Dual-colour imaging with GFP variants, *Trends Cell Biol.* 9, 52–56
7 Wu, P. and Brand, L. (1994) Resonance energy transfer: methods and applications, *Anal. Biochem.* 218, 1–13
8 Clegg, R.M. (1996) Fluorescence resonance energy transfer, in *Fluorescence Imaging Spectroscopy and Microscopy* (Wang, X-F. and Herman, B., eds), pp. 179–252, John Wiley & Sons
9 Pollok, B.A. and Heim, R. (1999) Using GFP in FRET-based applications, *Trends Cell Biol.* 9, 57–60
10 Gordon, G.W. *et al.* (1998) Quantitative fluorescence resonance energy transfer measurements using fluorescence microscopy, *Biophys. J.* 74, 2702–2713
11 Gadella, T.W.J., Jr and Jovin, T.M. (1995) Oligomerization of epidermal growth factor receptors (EGFR) on A431 cells studied by time-resolved fluorescence imaging microscopy. A stereochemical model for tyrosine kinase receptor activation, *J. Cell Biol.* 129, 1543–1558
12 Bastiaens, P.I.H. and Squire, A. (1999) Fluorescence lifetime imaging microscopy: spatial resolution of biochemical processes in the cell, *Trends Cell Biol.* 9, 48–52
13 Gadella, T.W.J., Jr (1999) Fluorescence lifetime imaging microscopy (FLIM): instrumentation and applications, in *Fluorescent and Luminescent Probes for Biological Activity. A Practical Guide to Technology for Quantitative Real-time Analysis* (2nd edn) (*Biological Techniques Series*) (Mason, W.T., ed.), pp. 467–479, Academic Press
14 Miyawaki, A. *et al.* (1997) Fluorescent indicators for Ca^{2+} based on green fluorescent proteins and calmodulins, *Nature* 388, 882–887
15 Miyawaki, A. *et al.* (1999) Dynamic and quantitative Ca^{2+} measurements using improved cameleons, *Proc. Natl. Acad. Sci. U. S. A.* 96, 2135–2140
16 Gadella, T.W.J., Jr *et al.* (1997) Microspectroscopic imaging of nodulation factor-binding sites on living *Vicia sativa* roots using a novel bioactive fluorescent nodulation factor, *Biophys. J.* 72, 1986–1996
17 Wymer, C.L., Bibikova, T.N. and Gilroy, S. (1997) Cytoplasmic free calcium distributions during the development of root hairs of *Arabidopsis thaliana*, *Plant J.* 12, 427–439
18 Mahajan, N.P. *et al.* (1998) Bcl-2 and Bax interactions in mitochondria probed with green fluorescent protein and fluorescence resonance energy transfer, *Nat. Biotechnol.* 16, 547–552
19 Xu, X. *et al.* (1998) Detection of programmed cell death using fluorescence energy transfer, *Nucleic Acids Res.* 26, 2034–2035
20 Miesenböck, G., De Angelis, D.A. and Rothman, J.E. (1998) Visualizing secretion and synaptic transmission with pH-sensitive green fluorescent proteins, *Nature* 394, 192–195

Poster on 'MADS-Box Genes and Plant Development'

This issue of *Trends in Plant Science* contains a fold-out poster detailing exciting recent research on MADS-box genes. The poster has been prepared by the laboratories of Marty Yanofsky and Bob Schmidt (Dept of Biology, University of California at San Diego, USA) and features their work on *Arabidopsis* and maize, respectively. Our thanks to all the laboratory members whose efforts have contributed to the poster, and to the sponsors, Qiagen.